Biochemical and Biophysical Research Communications 422 (2012) 128–132

Contents lists available at SciVerse ScienceDirect

Biochemical and Biophysical Research Communications

journal homepage: www.elsevier.com/locate/ybbrc

Role of side-edge site of sphingomyelinase from *Bacillus cereus*

Masataka Oda [a,*], Masaya Takahashi [a], Hideaki Tsuge [b,c], Masahiro Nagahama [a], Jun Sakurai [a]

[a] Department of Microbiology, Faculty of Pharmaceutical Sciences, Tokushima Bunri University, Yamashiro-cho, Tokushima 770-8514, Japan
[b] Institute for Health Sciences, Tokushima Bunri University, Yamashiro-cho, Tokushima 770-8514, Japan
[c] Faculty of Life Sciences, Kyoto Sangyo University, Kamigamo Motoyama Kita-ku, Kyoto 603-8555, Japan

ARTICLE INFO

Article history:
Received 18 April 2012
Available online 30 April 2012

Keywords:
Bacillus cereus
Sphingomyelinase
Side-edge site
Membrane binding

ABSTRACT

Bacillus cereus sphingomyelinase (*Bc*-SMase) belongs to the Mg^{2+}-dependent neutral sphingomyelinase (nSMase) which hydrolyzes sphingomyelin (SM) to produce phosphocholine and ceramide, and acts as an extracellular hemolysin. *Bc*-SMase has two metal ion-binding sites in a long horizontal cleft across the molecule, with one Mg^{2+} in the central region of the cleft and one divalent metal ion at the side-edge of the cleft. The role of the Mg^{2+} at the side-edge of the long horizontal cleft in *Bc*-SMase remains unresolved. The replacement of Asn-57, Glu-99, and Asp-100 located in close proximity to Mg^{2+} at the side-edge with alanine resulted in a striking reduction in binding to and hydrolysis of sphingomyelin in membranes of sheep erythrocytes or SM-liposomes but that of Phe-55 did not. However, the replacement of these residues had little effect on the enzymatic activity. N57A, E99A, and D100A contained 2 mol of Mg^{2+} per mol of protein, and the wild type and F55A contained 3 mol. A crystal analysis showed that N57A with Mg^{2+} had no metal ion at the side-edge. These results indicate that the Mg^{2+} at the side-edge of *Bc*-SMase plays an important role in the binding to membranes.

Published by Elsevier Inc.

1. Introduction

Sphingomyelinase (sphingomyelin phosphodiesterase; EC 3.1.4.12), which catalyzes the hydrolysis of sphingomyelin to produce phosphocholine and ceramide, is widely distributed from eukaryotes to prokaryotes. Eukaryotic SMases have been classified according to their pH as acid [1], alkaline [2], and neutral [3,4] SMase. In prokaryotes, some broad specificity phosphatidylcholine phospholipase C enzymes possess SM-hydrolyzing activity [5,6] but a number of pathogenic bacteria, such as *Staphylococcus aureus* (β-hemolysin [7,8]), *Bacillus cereus* [9], *Leptospira interrogans* [10], and *Listeria ivanovii* [11,12], produce SM-specific phospholipases. These bacterial SMases share sequence homology with the eukaryotic nSMases and have a similar catalytic mechanism and overall structure [13,14]. In addition, bacterial nSMases have specific amino acid residues unlike the enzymes from eukaryotes (Fig. 1).

Bc-SMase is one of a group of bacterial extracellular toxins, and exhibits potent hemolytic activity against SM-rich erythrocytes in mammals such as ruminants. We reported that divalent metal ions were effective in stimulating the activity of *Bc*-SMase in the order Co^{2+} > or = Mn^{2+} > or = Mg^{2+} >> Ca^{2+} > or = Sr^{2+}, and resolved the structure of *Bc*-SMase-bound Co^{2+}, Mg^{2+}, or Ca^{2+} [15]. The crystal analysis showed that *Bc*-SMase has two metal ion-binding sites in a long horizontal cleft across the molecule and that one Mg^{2+} or two Co^{2+} exist in the central region of the cleft, and one divalent metal ion exists at the side-edge of the cleft [15]. We also showed that the metal ion(s) in the central region plays an important role in the enzymatic activity of *Bc*-SMase [15]. In addition, we provided evidence that the exposed loop from Asn-92 to Pro-98 participates in the binding to the phosphorylcholine moiety of the substrate [15]. Several researchers reported that Glu-53, His-151, Asp-195, Asn-197, and His-296 at the central site participate in the hydrolysis of substrates [15–18]. However, little is known about the role of the side-edge, which is in a conserved sequence of the bacterial SMases, in the SMase and hemolytic activities of *Bc*-SMase.

In this study, we investigated the functional role of the side-edge as a metal ligand in the enzymatic action and binding to membranes of *Bc*-SMase.

2. Materials and methods

2.1. Preparation of Bc-SMase and variants

Bc-SMase was overexpressed in *B. subtilis* ISW1214 transformed with the plasmid vector pHY300PLK carrying cDNA of *Bc*-SMase cloned from *B. cereus* IAM1029. The expression and purification of the recombinant *Bc*-SMase and variant enzymes were performed as described previously [15].

2.2. Site-directed mutagenesis

The transformer site-directed mutagenesis kit (BD Biosciences, USA) was used with the primers F55A: 5′-TTAAATGAAGTGGCGGAT

* Corresponding author. Fax: +81 88 655 3051.
E-mail address: masa@ph.bunri-u.ac.jp (M. Oda).

0006-291X/$ - see front matter Published by Elsevier Inc.
http://dx.doi.org/10.1016/j.bbrc.2012.04.120

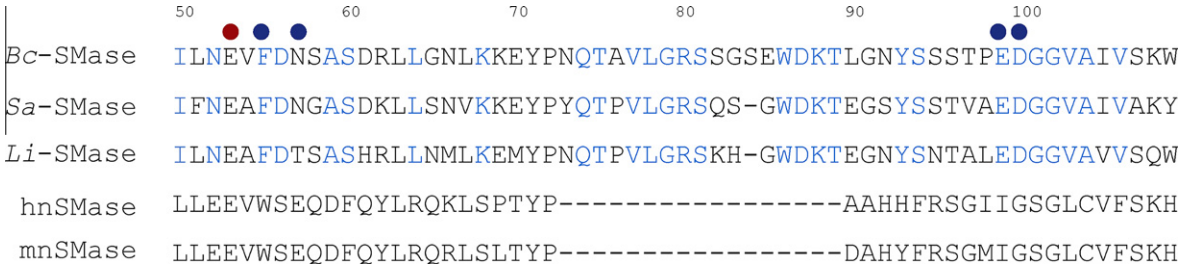

Fig. 1. The amino acid sequence alignment. The amino acid sequences of the magnesium-dependent neutral SMases from *B. cereus* (*Bc*-SMase), *S. aureus* (*Sa*-SMase), and *L. ivanovii* (*Li*-SMase), human neutral SMase (hnSMase), and mouse neutral SMase (mnSMase) were aligned by the program T-Coffee [22]. The amino acid residues conserved between bacterial SMases are indicated in sky blue. The amino acid residues participating at the central metal-binding site and side edge metal-binding site are shown by red circles and blue circles, respectively. (For interpretation of the references to colour in this figure legend, the reader is referred to the web version of this article.)

AATAGCGCT-3′, N57A: 5′-GAAGTGTTTGATGCGAGCGCTTCAGAT-3′, E99A: 5′-TCTTCAACTCCTGCGGATGGTGGCGTT-3′, D100A: 5′-TCAA CTCCTGAAGCGGGTGGCGTTGCG-3′, and E53A: 5′-GTTATTTTAAATG CCGTGTTTGATAATAGC-3′, to prepare the modified plasmid. The genetic sequence of *Bc*-SMase in each plasmid was confirmed with an ABI3500 PRISM™ genetic analyzer (Life technologies, USA).

2.3. Hemolytic activity assay

The hemolytic activity of the enzyme was determined by the amount of hemoglobin released from sheep erythrocytes using a method described previously [19]. The reaction mixture containing the enzyme at various concentrations, 3% (w/v) sheep erythrocytes, 20 mM Tris–HCl buffer (pH 7.5), 3 mM $MgCl_2$, and 0.9% (w/v) NaCl, was incubated for 30 min at 37 °C and then centrifuged at 500*g* for 3 min in order to prepare the test aliquot. Lysis was determined spectrophotometrically at A_{550nm}.

2.4. Preparation of SM-liposomes

Multilamellar SM-liposomes composed of SM and cholesterol were prepared according to previous reports [20].

2.5. SMase activity assay

SMase activity was measured using an Amplex Red Sphingomyelinase assay kit (Invitogen, USA). Liposome-disrupting activity was determined from the amount of carboxyfluorescein (CF) released in the test aliquot. The liposomes were incubated with *Bc*-SMase in 20 mM Tris–HCl (pH 7.5) containing 1 mM $MgCl_2$, and 0.9% (w/v) NaCl for 30 min at 37 °C. The wavelengths for excitation and measurement were 490 and 530 nm, respectively.

2.6. Binding of Bc-SMase and variant enzymes to SM-liposomes

SM-liposomes were incubated with the wild type and variant enzymes in the presence of 20 mM Tris–HCl (pH 7.5) and 0.9% (w/v) NaCl containing 5 mM $CaCl_2$ for 30 min at 37 °C. The binding to SM-liposomes was determined by SDS–PAGE and Western blotting using anti *Bc*-SMase antibody. A quantitative analysis of bands was performed by densitometry (LAS-3000, Fujifilm, Japan).

2.7. Detection of wild type or variant toxin binding to erythrocyte membranes

Erythrocyte membranes (5 mg of protein) in Tris-buffered saline were incubated with 1 mg of wild type or variant toxin in the presence or absence of 3 mM $CaCl_2$ at 37 °C for 30 min. After incubation, the membranes were collected by centrifugation at 15,000 rpm for 20 min. The pellet was washed twice with 3 ml of Tris-buffered saline (4 °C) and was centrifuged again. The pellet was dissolved in 20 μl of 20 mM Tris–HCl buffer (pH 7.5) containing 2% SDS, and the solution was boiled for 3 min. SDS–PAGE was performed on 12.5% gels, and the protein bands were then transferred to a polyvinylidene fluoride membrane (Immobilon P; Millipore, USA). The membrane was incubated first with polyclonal anti-*Bc*-SMase (rabbit) antiserum (diluted 1:1000) and then with horseradish peroxidase-conjugated anti-rabbit immunoglobulin G (Cell Signaling Technology; 1:1000). The wild type and variant toxins on the membrane were visualized with an enhanced chemiluminescence Western blot analysis system (Fujifilm, Tokyo, Japan).

2.8. Determination of amounts of Mg^{2+} and Co^{2+} in wild type and variant enzymes

The wild type and variant enzymes were chromatographed on a Sephadex G-25 column (10 by 1 cm; Pharmacia, Sweden) that was equilibrated with 20 mM Tris–HCl buffer (pH 7.5). Amounts of Mg^{2+} and Co^{2+} were determined using a Hitachi model Z-8200 atomic absorption spectrometer. The results obtained for each batch of wild type or variant toxins were averages of three or four determinations. All solutions were prepared in plasticware using Milli-Q-water (Millipore, USA) filtrated by a Chelex-100 column (Bio-Rad, USA).

2.9. Crystallization

The initial screening for crystallization of N57A was carried out using Crystal Screens (Hampton Research, USA) by the hanging-drop vapor-diffusion method at 4 °C. The crystal belonging to the space group $P2_12_12_1$ (cell dimensions of $a = 55.1$, $b = 63.9$, $c = 101.7$ Å and $\alpha = \beta = \gamma = 90$) was grown in hanging drops in which 2 μl of the enzyme solution (10 mg/ml N57A in 20 mM Tris–HCl (pH7.0)) was equilibrated against a reservoir containing 18% (w/v) polyethylene glycol 8000, 0.2 M $MgCl_2$, and 0.1 M sodium cacodylate (pH 6.5).

2.10. Data collection and processing

Data for the crystals were collected in-house (RAXIS/FR-E, Rigaku) to a resolution limit of 2.4 Å using cryo-conditions. Data were processed using an HKL 2000 and Scalepack.

2.11. Phasing and refinement

The crystal was in an asymmetric unit. The structure was solved by MOLREP and refined using XtalView and REFMAC5. Several cycles of refinement gave a final R_{cryst} and R_{free} of 18.4% and 23.5%, respectively. A Ramachandran plot analysis with PROCHECK showed that 87.6% of the residues in the current model were in

the most favorable region and no residue was in the disallowed region. The crystallographic statistics of the collected data and the refined models are summarized in Supplemental Table S1. PyMOL (DeLano Scientific LLC) was used to prepare the figures.

2.12. Coordinates

The coordinates and structural factors of N57A have been deposited in the Protein Data Bank with accession code 2UYR.

2.13. Statistic analysis

All data presented are expressed as the mean ± SEM. Comparisons of mean values among experimental groups were made with Student's *t*-test. $P < 0.05$ was considered statistically significant.

3. Results

3.1. Role of Phe-55, Asn-57, Glu-99, and Asp-100 in biological activities of Bc-SMase

The amino acid sequence of *Bc*-SMase is known to be homologous to that of the mammalian-derived SMases [8,12,15]. Therefore, we investigated the relationship between the structure and the function of *Bc*-SMase. The amino acid residues involved in the binding of divalent metal ions at the active site of *Bc*-SMase include Glu-53, Asp-195, Asn-197, Asp-295, and His-296 [15–17]. These residues are conserved in bacterial and mammalian nSMase. We reported that Phe-55, Asn-57, Glu-99, and Asp-100 in the proximity of Mg^{2+} at the side-edge are conserved in the bacterial nSMases (Fig. 1), but not in the mammalian nSMase [15]. To investigate the role of Phe-55, Asn-57, Glu-99, and Asp-100 in the activity of *Bc*-SMase, these residues were replaced with alanine by site-directed mutagenesis. The variants were incubated with sheep erythrocytes or liposomes composed of SM and cholesterol (SM-liposomes) containing CF at 37 °C for 30 min (Table 1). The hemolytic activity of N57A, E99A, and D100A was approximately 4.0%, 0.2%, and 0.1% of that of the wild type enzyme, respectively. The liposome-damaging activity of N57A, E99A, and D100A was approximately 6.0%, 0.2%, and 0.1%, respectively, of that of the wild type. However, replacement of Phe-55 with alanine had little effect on these activities (Table 1). The results show that the side chain of Asn-57, Glu-99, and Asp-100 is essential to these activities, but that of F55 is not. The SMase activity of these variants was measured using an Amplex Red Sphingomyelinase assay kit. As shown in Table 1, the replacement of Phe55, Asn57, Glu99, and Asp100 had little effect on SMase activity. The replacement of Glu-53, which binds to a divalent metal ion at the central site of the cleft, however, resulted in a loss of hemolytic and enzymatic activities (Table 1) under our experimental conditions, as reported previously [16]. The results showed that Asn-57, Glu-99, and Asp-100 play an important role in the disruption of biological and artificial membranes, but not the enzymatic activity.

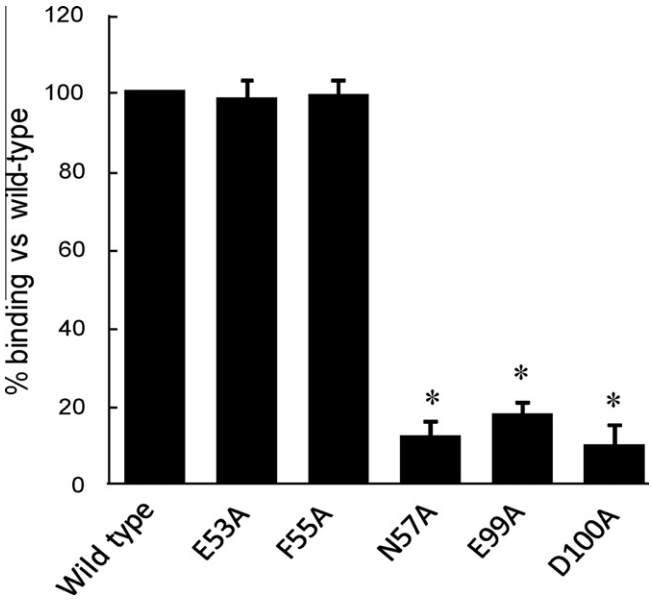

Fig. 2. Binding of wild type and variant enzymes to SM-liposomes. Wild type and variant enzymes were incubated with SM-liposomes in TBS containing 5 mM $CaCl_2$ for 30 min at 37 °C. The binding to SM-liposomes was determined by SDS–PAGE and Western blotting using anti-*Bc*-SMase antibody. The relative density of the bands was quantified by densitometry. The binding level of the wild type was set to 100%. Values are the mean ± SEM. ($n = 5$) $^*P < 0.005$ compared with binding of the wild type.

3.2. Binding of the wild type and variant enzymes to SM-liposomes

We tested whether or not the variants bind to SM-liposomes. The wild type and the variants were incubated with SM-liposomes at 37 °C for 30 min, and subjected to SDS–PAGE and Western blotting using the polyclonal anti-*Bc*-SMase antibody. The result indicated that the relative amount of E53A, F55A, N57A, E99A, and D100A bound to SM-liposomes was approximately 98%, 99%, 12%, 18%, and 10% of that of the wild type, respectively (Fig. 2), showing that N57A, E99A, and D100A did not bind to membranes of SM-liposomes. In addition, the binding of wild type *Bc*-SMase to the liposomes was completely inhibited by 1 mM EDTA. Furthermore, the binding of N57A, E99A, and D100A to sheep erythrocytes was lower than that of the wild type, F55A, and E53A (data not shown). It therefore appears that these residues directly or indirectly contribute to the binding.

3.3. Amounts of magnesium and cobalt ions in the wild type and variant enzymes

We reported that Mg^{2+} and Co^{2+} were effective in activating the enzymatic activity of *Bc*-SMase [15]. Therefore, the wild type and variant enzymes were incubated in 20 mM Tris–HCl buffer (pH 7.5) with 10 mM Mg^{2+} or Co^{2+}, and dialyzed in the buffer without

Table 1
Biological activities of variant enzymes.

Enzymes	Hemolytic activity (%)	CF-release from liposomes (%)	Sphingomyelinase activity (%)
Wild type	100	100	100
F55A	98.3 ± 2.1	99.2 ± 2.6	98.9 ± 3.9
N57A	1.1 ± 0.02	1.2 ± 0.03	97.1 ± 4.7
E99A	0.2 ± 0.07	0.2 ± 0.05	95.2 ± 2.1
D100A	0.1 ± 0.03	0.1 ± 0.04	94.7 ± 3.9
E53A	>0.01	>0.01	>0.01

Activity (%) was expressed as a percentage of each activity in the wild type enzyme. Each value is the mean for five experiments.

Table 2
Content of magnesium and cobalt ions in wild type and variant enzymes.

Enzymes	Magnesium ion	Cobalt ion
	(mol/mol of protein)[a]	
Wild type	3.01 ± 0.08	3.06 ± 0.11
F55A	2.96 ± 0.12	2.98 ± 0.09
N57A	2.12 ± 0.09	2.06 ± 0.13
E99A	2.03 ± 0.09	1.99 ± 0.08
D100A	1.95 ± 0.14	1.89 ± 0.11

[a] The amounts of magnesium and cobalt ions in the wild type and variant enzymes were determined by atomic absorption spectrophotometry as described in Section 2.

Mg^{2+} or Co^{2+}. The amounts of the divalent metal cations in these proteins were determined by using an atomic absorption spectrometer. Table 2 shows that the wild type and F55A contained about 3 mol of Mg^{2+} or Co^{2+} per mol of enzyme, and that N57A, E99A, and D100A contained about 2 mol of Mg^{2+} or Co^{2+} per mol of the variants. The metal ions were not detected in the EDTA-treated wild type, which possessed no hemolytic activity (data not shown). However, incubation of the EDTA-inactivated enzyme with Mg^{2+} or Co^{2+} resulted in a complete recovery of the activity, as reported by Ikezawa et al. [21], and restored the enzyme to 3 metal ions per mol (data not shown).

3.4. Analysis of the crystal structure of N57A

The N57A crystal with Mg^{2+} was solved at 1.8 Å. A comparison of the crystal structure of the wild type with that of N57A is shown in Fig. 3. The result showed that the overall structure of N57A was unaltered in the wild type reported previously (data not shown, PDB 2UYR), suggesting that the replacement of Asn57 had little effect on global and local change in the structure. As shown in Fig. 3, a close-up of the side-edge region revealed that the metal ion was not present in N57A, but the coordination of the metal ion at the center of the cleft of N57A was similar to that of the wild type. Therefore, it is apparent that N57A does not contain Mg^{2+} at the side-edge and has 2 mol of Mg^{2+} per mol of protein at the central site.

4. Discussion

The present study has demonstrated that the metal ion trapped by Asn-57, Glu-99 and Asp100 at the side-edge in *Bc*-SMase played an important role in binding to membranes. Analysis of the crystal form suggests that the side-edge metal ion is coordinated by Phe-55, Asn-57, Glu-99, and Asp-100 which are conserved in bacteria-derived nSMase [15]. Furthermore, one Mg^{2+} at the side-edge of the enzyme was detected by crystal structure analysis using X-ray in the wild type, but not in N57A. In addition, N57A, E99A, and D100A contained 2 mol of Mg^{2+}. Therefore it is apparent that N57A, E99A, and D100A do not contain Mg^{2+} at the side-edge. N57A, E99A, and D100A weakly bound to sheep erythrocytes and SM-liposomes, but had SMase activity, indicating that the metal ion surrounded by Asn-57, Glu-99, and Asp-100 plays a role in the binding to membranes, but not in the catalytic activity. The substitution of Asn-57, Glu-99, and Asp-100 with alanine caused a marked reduction in membrane-damaging activity, hemolysis of sheep erythrocytes, and leakage of CF from SM-liposomes. In addition, N57A, E99A, and D100A had little effect on mouse macrophages. The observations show that the binding of the side-edge to target cells is important to these biological activities of *Bc*-SMase. On the other hand, the substitution of Phe-55 had little effect on hemolytic and SMase activities and binding to the divalent metal ion. The crystal structure analysis suggested that the carbonyl oxygen of the peptide bond between Val-54 and Phe-55 coordinates with the metal ion of the side-edge, but the side chain does not attach to the metal ion [15]. The observation supports that the substitution of the residue results in little reduction in the activities of *Bc*-SMase. It therefore appears that the side chains of Asn-57, Glu-99, and Asp-100, and the main chain of Phe-55 coordinate with the metal ion of the side-edge. These observations show that the metal ion trapped by these residues at the side-edge plays an important role in binding to biological membranes.

The wild type enzyme and F55A in the buffer solution contained 3 mol of Mg^{2+} or Co^{2+} per mol of protein. On the other hand, N57A, E99A, and D100A contained 2 mol of the metal ion per mol of protein under the conditions, suggesting that one metal ion is lost in these variants. We reported that the crystal structure of *Bc*-SMase in complexes with Co^{2+} and Mg^{2+} contained two Co^{2+} and one Mg^{2+}, respectively, at the central site; the electron density of Co^{2+} in the crystal was defined on Glu53 (site A) and His296 (site B) at the central site, while that of Mg^{2+} was defined on Glu-53, but not on His-296. One Co^{2+} or one Mg^{2+} at the side-edge was detected in each crystal [15]. However, *Bc*-SMase in 20 mM Tris–HCl buffer (pH 7.5) containing Co^{2+} and Mg^{2+} included three mol of Co^{2+} and Mg^{2+} per mol of protein, respectively. Therefore, the number of Co^{2+} in the buffer was the same as that in the crystal, but the number of Mg^{2+} in the buffer was different from that in the crystal. The crystal analysis showed that the architecture of

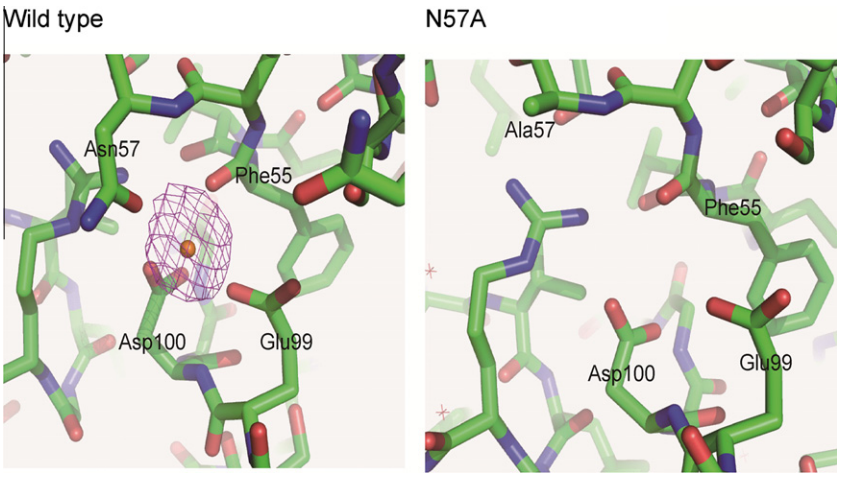

Fig. 3. Comparison of the structure of N57A and wild type *Bc*-SMase. The region of the side edge metal ion of the wild type (A) and N57A (B) is shown. The bound Mg^{2+} is represented by an orange sphere. This figure was rendered in PyMol. (For interpretation of the references to colour in this figure legend, the reader is referred to the web version of this article.)

the water molecules and amino acid residues (Asp-195, Asn-197, and His-296) at site B of the Co^{2+}-bound form coincided with that of the Mg^{2+}-bound form. Furthermore, in the anomalous difference Fourier map, the peak height of the Co^{2+} bound to Glu-53 at site A was much higher than that of the Co^{2+} bound to His-296 at site B, suggesting that site B has lower affinity for metal ions than site A [15] and that one Mg^{2+} is not trapped at site B of the crystal with Mg^{2+}. The crystal analysis strongly supported the notion that two metal ions bound to Glu-53 and His-296 serve as a foothold for holding SM in the proper orientation relative to the active site. The central site containing site A and site B is the catalytic site, as reported previously [15]. It therefore is reasonable that two magnesium ions were held at the central site in the buffer, as well as Co^{2+}.

In conclusion, the side-edge of *Bc*-SMase plays an important role in the binding to membranes.

Acknowledgments

The authors thank Keiko Kobayashi and Yuki Saito for technical assistance. This research was supported in part by a Grant-in-aid for Scientific Research from the Ministry of Education, Culture, Sports, Science and Technology of the Japanese Government, and SENRYAKU program (2009-2010) of MEXT.

Appendix A. Supplementary data

Supplementary data associated with this article can be found, in the online version, at http://dx.doi.org/10.1016/j.bbrc.2012.04.120.

References

[1] E.H. Schuchman, M. Suchi, T. Takahashi, K. Sandhoff, R.J. Desnick, Human acid sphingomyelinase. Isolation, nucleotide sequence and expression of the full-length and alternatively spliced cDNAs, J. Biol. Chem. 266 (1991) 8531–8539.
[2] R.D. Duan, L. Nyberg, A. Nilsson, Alkaline sphingomyelinase activity in rat gastrointestinal tract: distribution and characteristics, Biochim. Biophys. Acta 1259 (1995) 49–55.
[3] S. Tomiuk, K. Hofmann, M. Nix, M. Zumbansen, W. Stoffel, Cloned mammalian neutral sphingomyelinase: functions in sphingolipid signaling?, Proc Natl. Acad. Sci. USA 95 (1998) 3638–3643.
[4] K. Hofmann, S. Tomiuk, G. Wolff, W. Stoffel, Cloning and characterization of the mammalian brain-specific, Mg^{2+}-dependent neutral sphingomyelinase, Proc. Natl. Acad. Sci. USA 97 (2000) 5895–5900.
[5] C. Geoffroy, J. Raveneau, J.L. Beretti, A. Lecroisey, J.A. Vazquez-Boland, J.E. Alouf, P. Berche, Purification and characterization of an extracellular 29-kilodalton phospholipase C from *Listeria monocytogenes*, Infect. Immun. 59 (1991) 2382–2388.
[6] R.W. Titball, A.M. Fearn, E.D. Williamson, Biochemical and immunological properties of the C-terminal domain of the alpha-toxin of *Clostridium perfringens*, FEMS Microbiol. Lett. 110 (1993) 45–50.
[7] S.J. Projan, J. Kornblum, B. Kreiswirth, S.L. Moghazeh, W. Eisner, R.P. Novick, Nucleotide sequence. The beta-hemolysin gene of *Staphylococcus aureus*, Nucleic Acids Res. 17 (1989) 3305.
[8] M. Huseby, K. Shi, C.K. Brown, J. Digre, F. Mengistu, K.S. Seo, G.A. Bohach, P.M. Schlievert, D.H. Ohlendorf, C.A. Earhart, Structure and biological activities of beta toxin from *Staphylococcus aureus*, J. Bacteriol. 189 (2007) 8719–8726.
[9] A. Yamada, N. Tsukagoshi, S. Udaka, T. Sasaki, S. Makino, S. Nakamura, C. Little, M. Tomita, H. Ikezawa, Nucleotide sequence and expression in Escherichia coli of the gene coding for sphingomyelinase of *Bacillus cereus*, Eur. J. Biochem. 175 (1988) 213–220.
[10] R.P. Segers, A. van der Drift, A. de Nijs, P. Corcione, B.A. van der Zeijst, W. Gaastra, Molecular analysis of a sphingomyelinase C gene from Leptospira interrogans serovar hardjo, Infect. Immun. 58 (1990) 2177–2185.
[11] B. Gonzalez-Zorn, G. Dominguez-Bernal, M. Suarez, M.T. Ripio, Y. Vega, S. Novella, J.A. Vazquez-Boland, The smcL gene of *Listeria ivanovii* encodes a sphingomyelinase C that mediates bacterial escape from the phagocytic vacuole, Mol. Microbiol. 33 (1999) 510–523.
[12] A.E. Openshaw, P.R. Race, H.J. Monzo, J.A. Vazquez-Boland, M.J. Banfield, Crystal structure of SmcL, a bacterial neutral sphingomyelinase C from *Listeria*, J. Biol. Chem. 280 (2005) 35011–35017.
[13] F. Rodrigues-Lima, A.C. Fensome, M. Josephs, J. Evans, R.J. Veldman, M. Katan, Structural requirements for catalysis and membrane targeting of mammalian enzymes with neutral sphingomyelinase and lysophospholipid phospholipase C activities. Analysis by chemical modification and site-directed mutagenesis, J. Biol. Chem. 275 (2000) 28316–28325.
[14] F.M. Goni, A. Alonso, Sphingomyelinases: enzymology and membrane activity, FEBS Lett. 531 (2002) 38–46.
[15] H. Ago, M. Oda, M. Takahashi, H. Tsuge, S. Ochi, N. Katunuma, M. Miyano, J. Sakurai, Structural basis of the sphingomyelin phosphodiesterase activity in neutral sphingomyelinase from *Bacillus cereus*, J. Biol. Chem. 281 (2006) 16157–16167.
[16] T. Obama, Y. Kan, H. Ikezawa, M. Imagawa, K. Tsukamoto, Glu-53 of *Bacillus cereus* sphingomyelinase acts as an indispensable ligand of Mg^{2+} essential for catalytic activity, J. Biochem. 133 (2003) 279–286.
[17] T. Obama, S. Fujii, H. Ikezawa, K. Ikeda, M. Imagawa, K. Tsukamoto, His151 and His296 are the acid-base catalytic residues of *Bacillus cereus* sphingomyelinase in sphingomyelin hydrolysis, Biol. Pharm. Bull. 26 (2003) 920–926.
[18] Y. Matsuo, A. Yamada, K. Tsukamoto, H. Tamura, H. Ikezawa, H. Nakamura, K. Nishikawa, A distant evolutionary relationship between bacterial sphingomyelinase and mammalian DNase I, Protein Sci. 5 (1996) 2459–2467.
[19] S. Ochi, M. Oda, H. Matsuda, S. Ikari, J. Sakurai, *Clostridium perfringens* alpha-toxin activates the sphingomyelin metabolism system in sheep erythrocytes, J. Biol. Chem. 279 (2004) 12181–12189.
[20] M. Oda, M. Takahashi, T. Matsuno, K. Uoo, M. Nagahama, J. Sakurai, Hemolysis induced by *Bacillus cereus* sphingomyelinase, Biochim. Biophys. Acta 1798 (2010) 1073–1080.
[21] H. Ikezawa, M. Matsushita, M. Tomita, R. Taguchi, Effects of metal ions on sphingomyelinase activity of *Bacillus cereus*, Arch. Biochem. Biophys. 249 (1986) 588–595.
[22] C. Notredame, D.G. Higgins, J. Heringa, T-Coffee: A novel method for fast and accurate multiple sequence alignment, J. Mol. Biol. 302 (2000) 205–217.